Catalytic, Conductive Bipolar Membrane Interfaces through Layer-by-Layer Deposition for the Design of Membrane-Integrated Artificial Photosynthesis Systems

Catalytic, Conductive Bipolar Membrane Interfaces via Layer-by-Layer Deposition for the Design of Membrane-Integrated Artificial Photosynthesis Systems

Michael B. McDonald,[a] Michael S. Freund*[b] and Paula T. Hammond*[a]

Abstract: In the presence of an electric field, bipolar membranes (BPMs) are capable of initiating water disassociation (WD) within the interfacial region, which can make water splitting for renewable energy in the presence of a pH gradient possible. In addition to WD catalytic efficiency, there is also need for electronic conductivity in this region for membrane-integrated artificial photosynthesis (AP) systems. Graphene oxide (GO) has been shown to catalyze WD and to be controllably reduced, resulting in electronic conductivity. Layer-by-layer (LbL) film deposition has been employed to improve GO film uniformity in the interfacial region to enhance WD catalysis and, through the addition of a conducting polymer in the process, add electronic conductivity in a hybrid film. Three different deposition methods were tested in order to optimize conducting polymer synthesis with oxidant in a metastable solution and yield the best film properties. It was found that an approach that includes substrate dipping in a solution containing the expected final monomer-oxidant ratio provides the most predictable film growth and smoothest films (by UV-visible spectroscopy and AFM/SEM, respectively), while dipping when the oxidant is in excess or co-spraying the oxidant and monomer produce heterogeneous films. Optimized films are electronically conductive, producing a membrane ohmic drop that is acceptable for AP applications. Films were integrated into the interfacial region of BPMs and reveal superior WD efficiency ($\geq$ 1.4 V @10 mA/cm^2) for thinner films (< 10 bilayers $\approx$ 100 nm) compared to both pure GO catalyst and conducting polymer individually, indicating that there is a synergistic effect between these materials in the structure configured by the LbL method.

[a] Dr. M. B, McDonald, Prof. P. T. Hammond*
Department of Chemical Engineering
Massachusetts Institute of Technology
77 Massachusetts Ave. Cambridge, MA 02139 (USA)
E-mail: Hammond@mit.edu

[b] Prof. M. S. Freund*
Department of Chemistry
Florida Institute of Technology
150 W. University Blvd. Melbourne, FL 32901 (USA)
E-mail: Michael.Freund@fit.edu

Supporting information for this article is given via a link at the end of the document.

Introduction

Bipolar membranes (BPMs) consist of an anion-exchange and a cation-exchange material laminated together, which produces a built-in potential across the layer interface. When placed in an electrochemical cell (e.g. in series between electrolyte and electrodes) in reverse-bias configuration, ion migration through the membrane is attenuated by the like-charge of the ion-exchange layers (Figure 1A).[1] This further increases the electric field (~10^8 V m^{-1}), initiating water dissociation (WD), forming OH^- and H^+ that migrate to the electrodes to neutralize charge and complete the circuit.[2,3] The unique pathway for ions in the electrolyte phase that involves OH^-/H^+ production makes several applications possible; namely, electrodialysis for the concentration of acids and bases.[4]

Recently, it has been proposed that BPMs can be used to maintain a steady-state pH gradient for electrosynthesis, such as H_2 for renewable energy via electrolysis of water,[5] as depicted in Figure 1. For this, a pH gradient is critical because the anodic process (the oxygen-evolution reaction, OER) and cathodic process (the hydrogen-evolution reaction, HER) are facilitated in high and low pH, respectively (Table 1). The electrode materials associated with OER and HER also tend to be stabilized in different pH, enabling the incorporation of more abundant, non-precious metal-based electrocatalysts.[6] Further, for designs that include light-absorbing components residing in solution (and therefore semiconductor-liquid boundaries) to generate H_2 directly from sunlight (artificial photosynthesis, AP), the associated materials are also stabilized in base and acid for the hole- (OER) and electron- (HER) generating processes.[7]

For an electrochemical configuration that includes a high-pH anode and low-pH cathode augmented by a BPM, the large decrease to the overall thermodynamic potential to -0.40 V from -1.23 V for a uniform pH system (Table 1) is offset by the WD thermodynamic potential of -0.83 V.[8] With two-thirds of the system potential shifted to the BPM WD process, minimizing WD overpotential becomes critical. Improved kinetics through engineering of the layer structural features as well as the addition of foreign catalytic materials can accomplish this, and significant efforts have been made using metallic, organometallic, polymeric and other macromolecular materials.[5] We have previously reported efficient BPMs made by spin-coating graphene oxide (GO, Figure 2A) onto commercially available anion-exchange membranes and then covering with Nafion proton-exchange membrane.[9]

One AP design of interest involves high aspect ratio-structured photoelectrodes directly embedded into a polymer electrolyte membrane (Figure 1B).[10] In this membrane-integrated AP construct, the membrane serves as a structural support, product separator, electrolyte and, in the absence of an external electric circuit, electron conductor. Previous approaches to meet these stringent requirements include the design of composites containing components with complementary functions.[11,12] To implement a BPM into membrane-integrated AP therefore, the membrane must account for these qualities in addition to WD catalysis. One previous approach innovates the GO-BPM for this purpose by controllably reducing GO (rGO) post-deposition, which restores some sp^2- carbon character and therefore conductive properties to graphene while leaving some

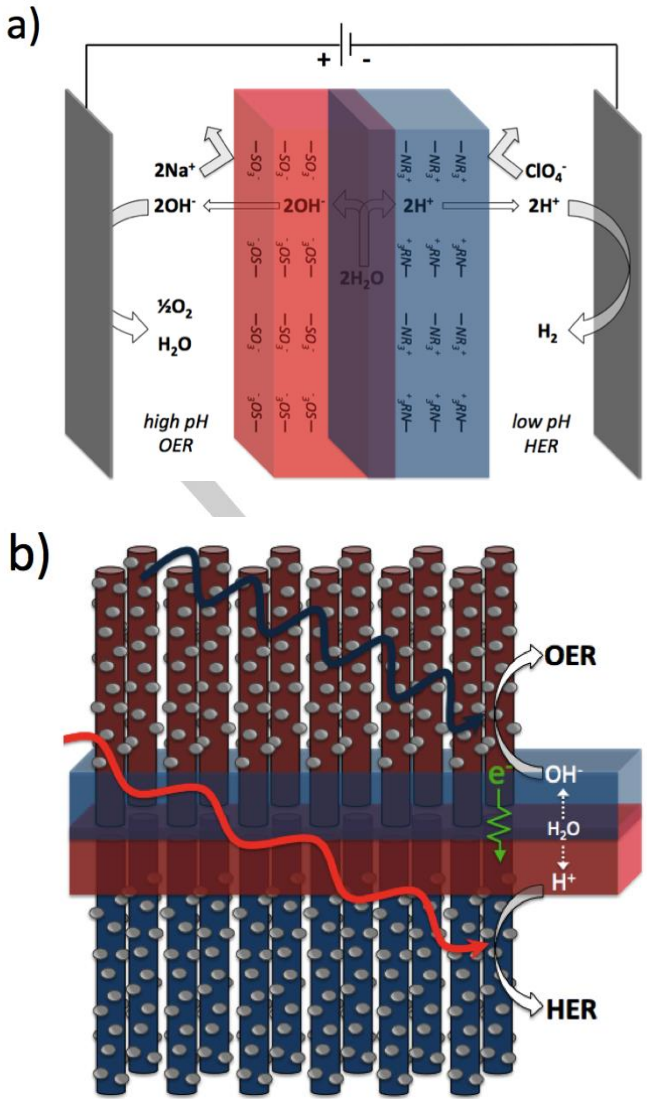

Figure 1. a) A BPM incorporated in a reverse bias electrochemical configuration with anode and cathode in high and low pH aqueous environments, respectively; b) conceptual BPM-integrated artificial photosynthesis design, containing catalyst-decorated, high-aspect ratio microphotoelectrodes embedded in a BPM, facilitating simultaneous high pH OER and low pH HER with charges (OH^-, H^+ and electrons) traversing the membrane.

catalytic functional groups.[13] The catalytic/conductor component tradeoff could be optimized by adjusting the chemical reduction conditions.

While the graphene BPM interface proved to significantly enhance WD and offered the potential to provide conductive properties, the spin-coat deposition method does not lead to high levels molecular orientation in these films, and the interfaces between materials is not uniform or well-defined. It has been reported that the structure of the interface, including molecular orientation and roughness, impact WD in terms of forming efficient pathways for water and ions, distributing the active catalytic sites, and maximizing the electric field intensity.[14-16] For these same reasons, the interface thickness is also very important, and also cannot be controlled on the

Table 1. Water electrolysis half-reactions and associated standard potentials (vs (H^+/H_2) at high and low pH.

	OER	HER
Low pH	$H_2O \rightarrow ½O_2 + 2H^+ + 2e^-$ (-1.23 V)	$2H^+ + 2e^- \rightarrow H_2$ (0.00 V)
High pH	$2OH^- \rightarrow ½O_2 + H_2O + 2e^-$ (-0.40 V)	$H_2O + 2e^- \rightarrow ½H_2 + OH^-$ (-0.83 V)

molecular scale using spin-coating. Therefore, improving control over the deposition process can optimize the structure formed. Lastly, the introduction of conductive properties comes at the expense of catalytic performance for rGO-BPMs, compromising the properties afforded by more heavily oxidized GO.

The aforementioned shortcomings in controlling film structure, film thickness, and introducing conductivity can be largely improved upon by nanostructuring the BPM interfacial layer using layer-by-layer (LbL) film deposition.[17] In this method, films are constructed by adsorption onto a substrate via electrostatic attraction of materials of alternating charge. Generally, an initially charged substrate is exposed to a solution containing a material of opposing charge, followed by a rinse step to remove excess material. The substrate is then exposed to a second solution containing a material that is once again oppositely charged, and the process is repeated to generate the desired functional thin film (Scheme 1). Deposition from dilute solutions can yield molecularly uniform of films, and the film thickness can be controlled on the nanoscale by the number of deposition cycles. The use of polyelectrolytes increases ion-exchange capacity, which both increases hydrophilicity for water replenishment and increases the magnitude of the electric field available to dissociate water molecules by creating a denser region of charges.[18] This method has been previously employed for significantly enhancing WD in BPMs using alternating polyelectrolyte catalysts.[19]

The duality of the LbL technique, in that at least one positive and one negative material is required, corresponds with the integration requirement for both a catalyst and conductor at the BPM interface. As noted, GO is an exceptional WD catalyst, and is negatively ionizable due to O-containing groups such as carboxylates and alcohols[20] that can exchange with positive materials. It would thus be ideal if GO were to be deposited via LbL in alternation with an electronic conductor that is positively charged to form a hybrid film. Charged polymers are highly utilized LbL materials that can be used to produce flat, uniform, and flexible films,[21] and can temper the rougher deposition of 2D nanomaterials such as GO,[22] clays,[23] and complex biomolecules.[24] Highly conjugated polymers contain long-range sp^2 carbon pathways, resulting in electronic conductivity: conducting polymers.[25] Among the most stable and processible conducting polymers is poly(3,4-ethylenedioxythiophene) (PEDOT, Figure 2B), which is p-doped and therefore contains delocalized positive charge along its conjugated backbone, balanced by an anionic dopant.[26] PEDOT is not water soluble alone, but is often synthesized with a large excess of poly(styrenesulfonic acid) (PSS) ("PEDOT:PSS") that acts as the

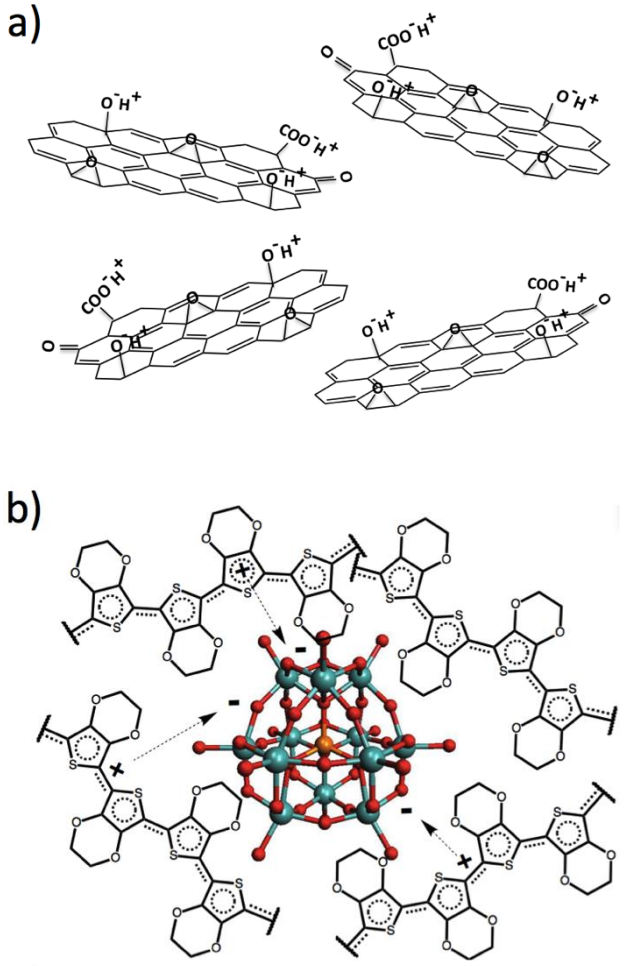

Figure 2. General chemical structure of a) GO and b) PEDOT-PMA. PEDOT segments with delocalized positive charge coordinate to the negative oxygen atoms (red) of PMA (blue: molybdenum, orange: phosphorus).

dopant, yielding a water-dispersible complex.[27] However, this process renders the formulation net-negative,[28] and so it is not suitable as an LbL pairing with GO. PSS can be replaced; however, *in situ* polymerization of the monomer EDOT using common oxidants such as $FeCl_3$ results in a rapid reaction with large polymer precipitates, due to polymer insolubility,[29,30] which are unsuitable for LbL processing.

Metastable solutions of PEDOT have been reported using *in situ* polymerization by heteropoly acids such as phosphomolybdic acid (PMA) as the oxidant and dopant ("PEDOT:PMA") (Figure 2B).[31] This polymer complex system, which has a net positive charge, was also previously investigated for application integrated AP membranes and was found to have excellent conductivity and stability as a function of pH.[32] In this work, the negatively charged WD catalyst GO is co-deposited with the positively charged PEDOT conductor that is formed *in situ* from a metastable solution of monomer with PMA, using an LbL procedure to produce a molecularly tailored, stable, conductive, and catalytic BPM interface of controllable thickness: "GO/PEDOT". Variations of the methodology, including polymerization conditions and deposition technique,

are explored to optimize the WD catalysis efficiency in an electrochemical system.

Results and Discussion

Evaluation of LbL Deposition. The procedure for formation of GO/PEDOT films by LbL involves the *in situ* synthesis of PEDOT-PMA, for which variables such as reaction time and monomer-oxidant ratios must also be considered. Therefore, three different LbL procedures were designed and tested to find the optimal conditions, which ultimately are determined by the resulting WD catalytic performances and are affected by the quality and controllability of the films formed. First, reaction time was probed using the co-spray method (Scheme 1b), where relatively short (~10 s) exposures to coating solutions were employed. Here, EDOT and PMA are sprayed in unison, and so PEDOT-PMA is presumably formed directly on the anion-exchange membrane or whilst airborne immediately before deposition. The combination of low concentration (~10^{-2} M) and high concentration ratio (10:1) of EDOT:PMA, as well as allowing only 1 min for the reaction to occur, safeguards against non-electrostatic accumulation of multilayers (non-LbL). By design, PMA is the limiting reactant and so excess PMA associating with the positively charged anion-exchange membrane will not dominate the film, and the immediate association by the positively charged PEDOT to the previous GO layer is likely preferred to PMA. Additionally, spray deposition is considered to produce more uniform films compared to the dip method for exposures on the seconds scale.[33] The dip method was used to both confirm the validity of these concerns, as well as probe the effect of reactant concentration. Two solution compositions were designed, both containing higher concentrations than the co-spray method (~10^{-1} M). 2:3 EDOT:PMA ("2:3 dip") was first selected to represent the scenario when the oxidant is in excess, as well as for its successful synthesis in previous work,[31, 32] while 4:1 EDOT:PMA ("4:1 dip") was designed based on the incorporation of one PMA unit in the PEDOT matrix for every four EDOT units ('rationalized approach').[31]

To test the effectiveness of the above three methods, as well as the ability to form the GO/PEDOT BL system in general, films were generated on glass substrates and their growth tracked by UV-visible absorbance spectroscopy. The co-spray method clearly shows the increasing magnitude of the absorbance spectrum as a function of the number of BLs (Figure 3A), indicating progressive film growth. Inset in Figure 3A is the additive spectrum of thicker, drop-cast pure GO plus pure PEDOT-PMA, which contains a maximum absorbance approaching the UV range for both components, as well as a broad trough with a minimum at ~480 nm and shoulder centered about ~700 nm associated with PEDOT-PMA. The measured spectra for the LbL GO/PEDOT morph into traces with similar features, indicating the successful deposition of both components. The same is true for films generated using the 2:3 (EDOT:PMA) dip method (Figure 3B); however, the absorbance is greater for less BLs than co-sprayed films, especially at low (≤ 10 BL) loadings. This could signify that the initial stage of the co-spray method results in films that do not saturate the surface charges, or there is an equilibration period to develop a foundation suitable for more predictable deposition. This may also be the case in the 2:3 dip experiment, where the absorbance of 1 BL is larger than subsequent depositions at < 400 nm, and so some condition at the substrate-film interface gives rise to unpredictable LbL growth at early stages. For the 4:1 dip method (Figure 3C), the increase in the absorbance spectra shows a predictable, progressive growth pattern also with greater absorbance, as observed for a 4 BL-thick film. Film growth is more linear with this method compared to the 2:3 dip method, where early deposition of material results in a greater

Scheme 1. LbL deposition of GO/PEDOT films using the a) dip and b) co-spray methods.

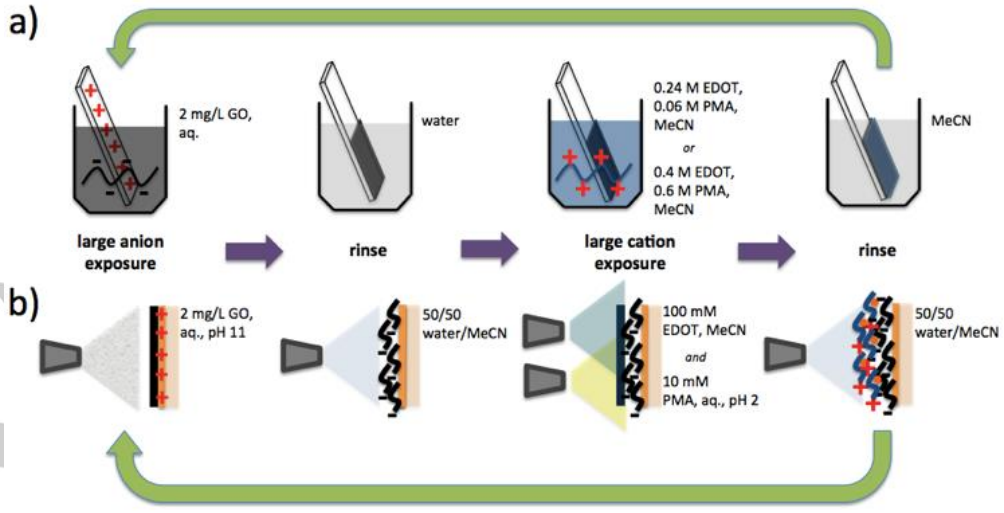

absorbance, with marginal gains for further repeated exposures. The lower absorbance for < 4 BLs implies thinner layers and therefore improved binding of the components to the substrate surface compared to the 2:3 dip method, and will likely result in better LbL growth due to reduced shielding.[34] This suggests that this 'rationalized' method affords the most effective and predictable LbL deposition of the procedures tested. Due to the high volatility of acetonitrile, deposition of films via drying may be possible. To verify that the increase in absorbance as a function of solution exposures is legitimate LbL deposition and not simply the physical (non-electrostatic) accumulation of material, the experiment was performed in the absence of GO (Figure 3D, and inset). The absorbance does not significantly increase and is not correlated to the number of layers attempted, confirming the authenticity of the LbL methodology designed here.

Films of conducting polymer synthesized using oxidation by a heteropoly acid tend to immobilize a stoichiometric amount of this oxidant with respect to charge balance in the matrix.[31] This LbL method differs in that the positively charged PEDOT that is deposited is coordinated to the negative charges on previously deposited GO. To examine if PMA is also incorporated into these films, XPS analysis was performed on films deposited via the 4:1 dip method (Figure S1). The ratio of phosphorous in PMA to sulfur in PEDOT was calculated for a 20 BL film and 100 BL film based on the P2p and S2p peaks, for which there is no overlap. The 100 BL sample showed a P:S ratio of ~3:1, and given 1 P and 1 S atom per molecular unit, this indicates there is a excessive amount of PMA trapped in this film. This could be due to aging of the metastable solution throughout the deposition process, forming longer PEDOT chains that may aggregate and physically entangle excess PMA molecules and immobilize them in later layers, which would be especially visible in surface-sensitive XPS. This reveals a limitation to film quality in the experimental procedure as a function of time if very thick films are desired. In contrast, the 20 BL sample indicates a similar presence of sulfur but not phosphorous, signifying that no PMA is incorporated in GO/PEDOT for this number of BLs and presumably less BLs. Because the BPM interface functionality is expected to be sensitive to modulation on the nanoscale,[14] thinner films (< 10 BLs) will be of interest, and thus no PMA is present.

The thickness of films constructed using the 4:1 dip method as a function of number of BLs deposited, and how they are related to their UV-vis absorbance, is shown in Figure 4. Thinner film systems (< 10 BLs) have an approximately linear increase in absorbance as a function of BLs deposited, with the

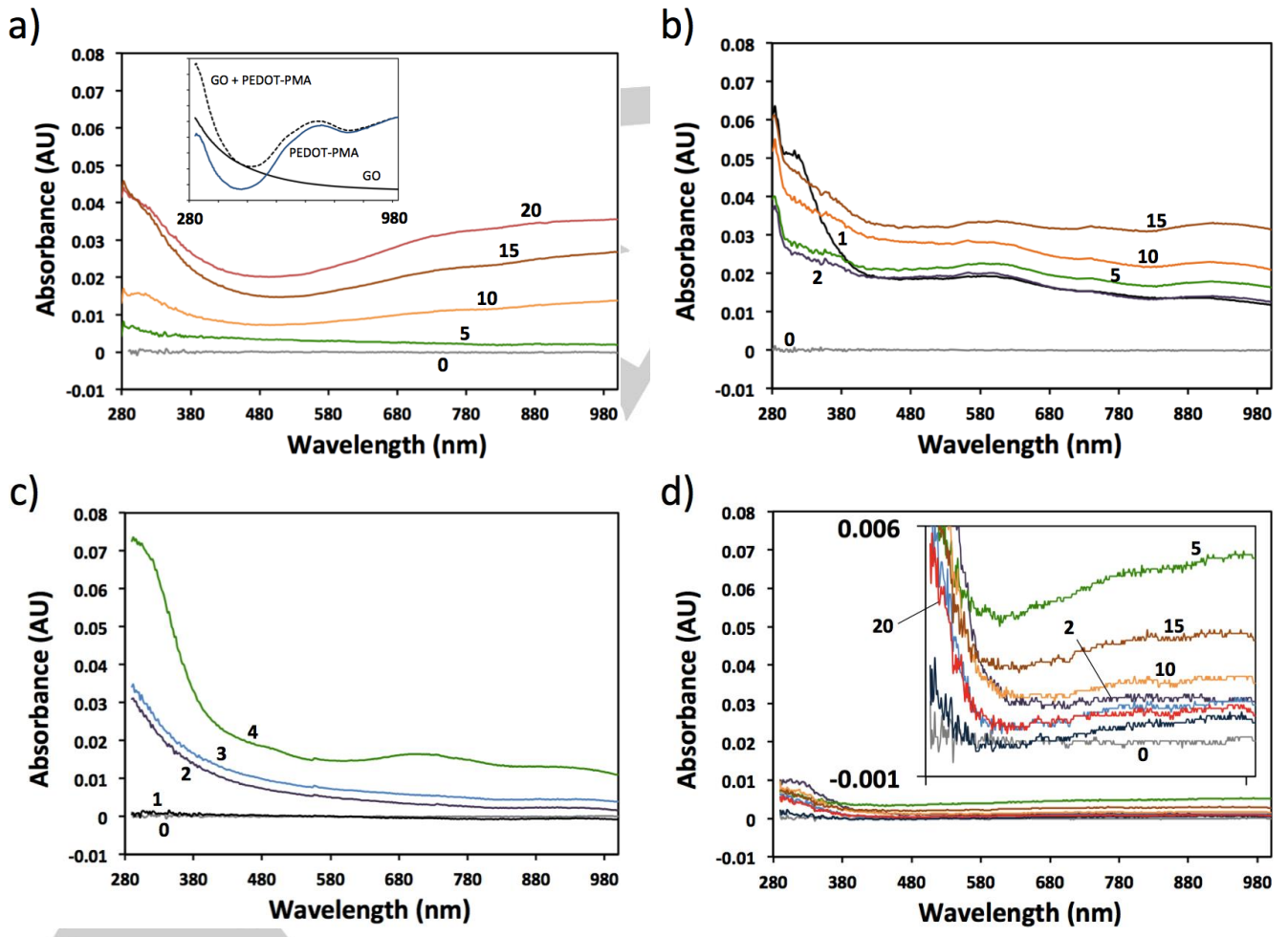

Figure 3. UV-visible spectra of varying GO/PEDOT BLs (numeral labels) deposited by LbL deposition on plasma-treated glass using the a) co-spray (inset: additive spectra of PEDOT-PMA and GO, colors do not apply), b) 2:3 dip and c) 4:1 dip methods. Also shown are films attempted to be deposited in the absence of GO using repeated immersions in 4:1 EDOT:PMA.

exception of the 6 BL, where there is a decrease. This result is not unexpected, as spectra shown in Figure 3 indicate non-uniformity in film deposition at the earlier stages, perhaps because of dissolution of loosely bound monolayers until a stable foundation is formed (note that 6 BL using the 4:1 dip method was not examined in Figure 3). For thickly layered films (10 – 100 BLs), the absorbance levels off, implying an increasing shielding to electrostatic binding due to the larger amount of material including PMA as confirmed by XPS, and therefore film build-up becomes less successful each cycle. Both absorbance at 325 nm and 750 nm were monitored to represent the GO- and PEDOT-dominated regions of the absorbance spectrum, respectively (see Figure 3a inset). In the thinner film regime, the higher absorbance tends to occur at 325 nm, which contains significant contributions from both the GO and PEDOT components, implying that both GO and PEDOT incorporate in an alternating fashion as intended. This is also in agreement with the XPS analysis, which showed no PMA inclusion in this regime and hence PEDOT coordination solely to GO. In the thicker film regime, the 750 nm absorbance tends to dominate, which is more largely associated with PEDOT-PMA. This is also in agreement with XPS in that the film includes PMA, and the implication that film build-up is inefficient for thicker films as GO is deposited less proportionately. The measured film thickness is in good agreement with the spectroscopic findings, increasing linearly with < 10 BL film loadings, and approaching a limit in very thick films. The purely GO/PEDOT LbL films are on the order of 100 nm thick, similar to the previously investigated spin-coated GO films.[9] This is two orders of magnitude greater than the calculated depletion region for astraight, abrupt junction of two homogeneous ion-exchange membranes in the absence of a catalytic layer.[35]

The quality of GO/PEDOT films formed by each method was evaluated using microscopy. AFM-phase micrographs of films on anion-exchange membrane are shown in Figure 5. This substrate was selected because the resulting film properties accurately reflect the interface qualities expected during fabrication into BPMs. Compared to the pristine anion-exchange membrane (Figure 5A), it is clear a film was deposited using the co-spray method; however, these films appear non-uniform and disheveled (Figure 5B). Anion-exchange

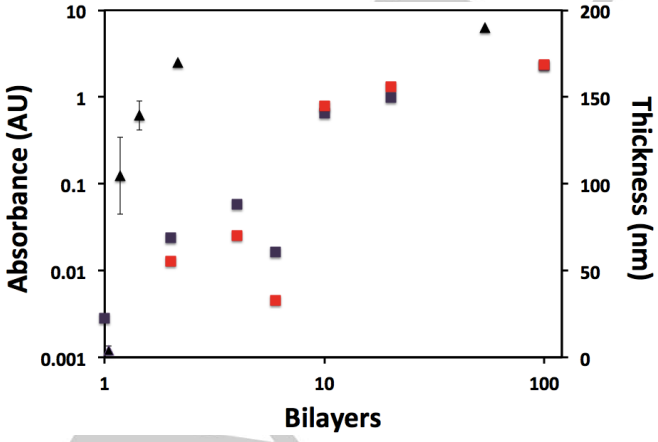

Figure 4. Film thickness (triangles) and UV-visible absorbance (squares) at 325 nm (purple) and 750 nm (red) as a function of number of GO/PEDOT BLs deposited via the 4:1 dip method.

membranes exposed to solutions with the 2:3 dip method do not show discernible differences compared to the bare membrane (Figure 5C). This is perhaps due to a lack of film building during early stages of LbL or a very thin but smooth film formed, as observed in the spectrometric findings. The 4:1 dip method produces a distinguishable and modestly smooth film with some cracking for only 1 BL (Figure 5D). Higher film loadings were also examined, with the co-spray method rendering a non-uniform, honeycomb-like film structure that is thick (as evidenced by the large color contrast) and heterogeneous at 5 BL (Figure 5E). By contrast, the 4:1 dip-treated anion-exchange membrane becomes smoother and more filled-in at 6 BLs compared to 1 BL (Figure 5F).

To gain more insight into the smoother, more homogeneous films produced by the dip methods, these films were also observed by SEM (Figure 6). Both the 1 BL and 6 BL films made by the 2:3 dip (Figure 6B–C) method are very heterogeneous, with flake accumulation that builds into a rough film for thicker layering, which were not observed in the geometrically smaller areas examined with AFM. Especially prominent is the formation of a separate string/mesh structure. Upon examining anion-exchange membrane with exposure to PEDOT-PMA solution only (Figure 6D), it is clear that it is the polymer that forms this morphology, implying that GO forms the flake/rough portion. It can be inferred that the excess oxidant in this method produces a more rapid, higher degree of polymerization such that macroscopic fibrous fragments are formed in the metastable solution and accumulate during the deposition. This lack of homogeneity and smoothness is theoretically unfavorable for the BPM interface. By contrast, the 4:1 dip produces highly smooth films with significantly less polymer/GO fragment accumulation, and therefore a large degree of homogeneity (Figure 6E–F). Based on all evidence gathered by spectroscopy and microscopy, with consideration of desired BPM interface properties, the 4:1 dip method produces morphologically superior films that grow predictably by verified LbL deposition and are expected to produce the desired alternating catalyst-conductor architecture afforded by this more rationalized approach.

Electronic Conductivity. Through-plane electronic conductivity measurements were performed in order to assess the feasibility of application of this BPM interfacial material to membrane-integrated electronics such as AP. A 10 BL and 100 BL film were tested and found to have a 10±3 Ω and 13±3 Ω film resistance (after accounting for junction resistance of the bare conductive substrates), respectively. The similarity between values despite significant differences in thickness implies that the overall resistance for these thin films does not differ discernibly. Assuming a thickness on the order of 100 nm (Figure 4), these films therefore have a conductivity of ~10^{-2} μS cm^{-1}. In the context of AP membranes, the ~10 Ω resistance is equivalent to a ~100 mV overpotential at the expected solar-induced current density of 10 mA cm^{-2} associated with the membrane component, which has been deemed as acceptable for efficient AP for H_2 production.[36]

Catalytic Performance. BPMs were fashioned by laminating Nafion (proton-conducting membrane) to treated (and untreated) anion-exchange membranes, and were tested for WD efficacy by effecting current via water electrolysis and measuring the voltage drop across the membrane. For this, neutral solution

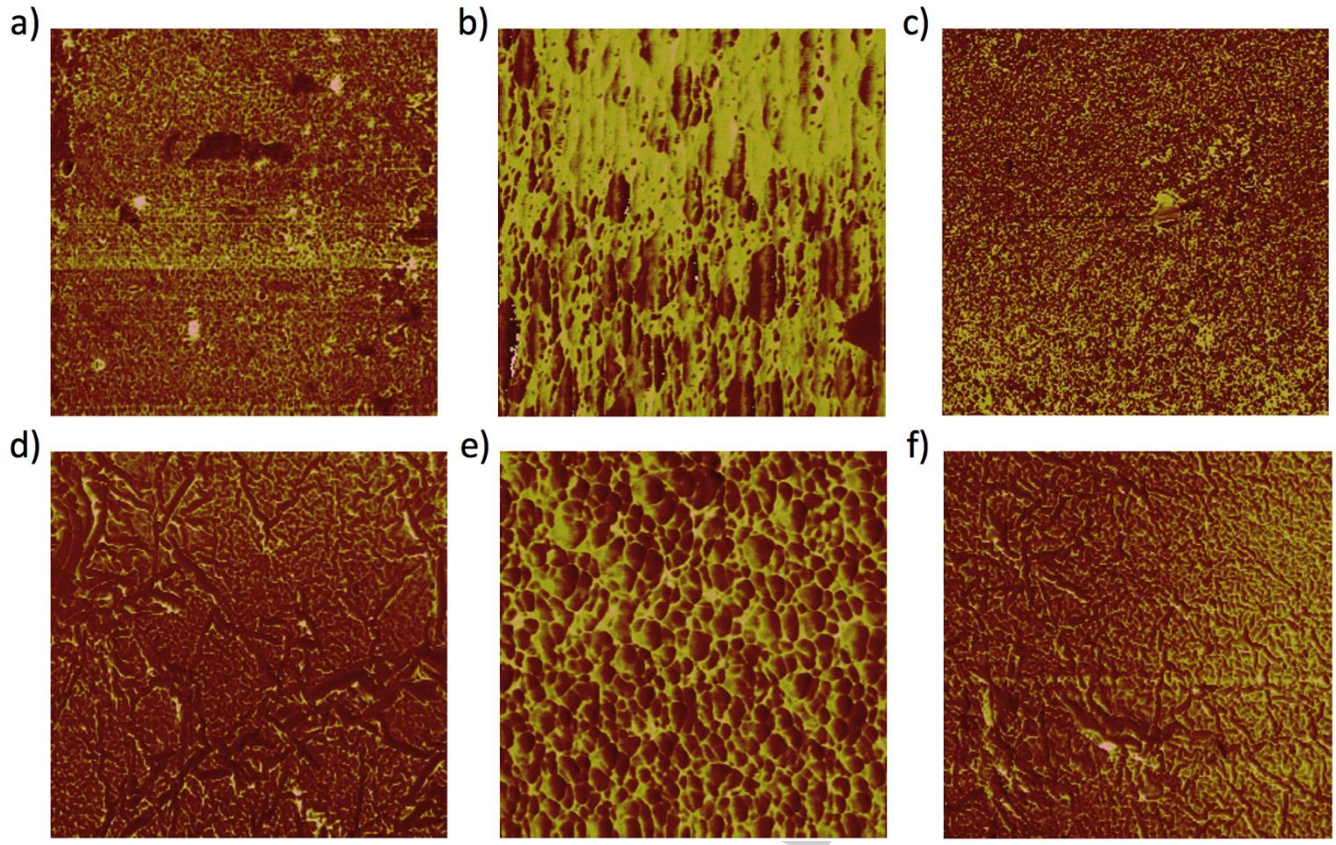

Figure 5. AFM-phase images of a) bare anion-exchange membrane (2 μm^2), and b) co-spray 2 BL (1 μm^2), c) 2:3 dip 1 BL (4 μm^2), d) 4:1 dip 1 BL (2 μm^2), e) co-spray 5 BL (1 μm^2) and f) 4:1 dip 6 BL (4 μm^2) GO/PEDOT on anion-exchange membrane.

containing inert electrolyte (1 M $NaClO_4$) was used rather than the proposed high pH OER/low pH HER configuration in order to observe the standard BPM current-voltage (*J-E*) relationship, which includes a ~0 V open-circuit potential reading rather than one caused by a pH difference, which is the traditional BPM condition.[37]

First, the individual contributions to WD by the anion-exchange membrane-Nafion interface, PEDOT, PMA, and GO were assessed using various deposition methods (Figure 7A). Thermodynamically, WD cannot be initiated at potentials < 0.83 V, and so the limited current in this region is leakage of ions of like charge with respect to the fixed membrane charge (i.e. Na^+ through anion-exchange membrane, ClO_4^- through Nafion) while the ohmic region at higher potentials is current passed via WD.[37] The untreated anion-exchange membrane-Nafion BPM produces a current onset at 2.4 V, with a gradual increase, indicating poor WD kinetics in the absence of membrane treatment/catalyst (3.9 V @ 20 mA/cm^2). A BPM interface containing only GO layers deposited using spray and dip methods (followed by immediate rinsing, congruent with LbL deposition), and spin-coating yield substantially more WD efficiency by comparison, regardless of method, with a current onset near 1 V and much steeper WD curves (2.4 – 2.5 V @ 20 mA/cm^2). This is in agreement with the previous work on GO-modified BPMs, showing vastly reduced overpotentials with minimal dependence on conditions, including interfacial layer thickness.[32] The improved kinetics in the presence of this thick layer relative to the calculated depletion region (region of high built-in voltage) suggest the catalytic effect transcends the limits of this domain; although, the relative roughness of the region means the field is likely spread much wider.[35] While XPS analysis implies no PMA is present in thinner films, an anion-exchange membrane was treated with only PMA using both spray and dip methods, as it is negatively charged it will presumably associate with the positively charged membrane surface. PMA is a known electrocatalyst for a variety of reactions[38] and so may be active should small quantities be present in GO/PEDOT, but the resulting BPM shows no difference from the untreated BPM, signifying that PMA is non-catalytic for WD regardless of deposition method. When the anion-exchange membrane is treated with only PEDOT-PMA using the spray method, the *J-E* response resembles the anion-exchange membrane-Nafion control. In contrast, when the deposition method is changed to dip-immersion, WD onset shifts near GO-initiated potentials and a curve slope closer to that of GO than the control BPM (2.7 V @ 20 mA/cm^2). This indicates that the conducting polymer is active in WD catalysis, and this is dependent on deposition method. For PEDOT-PMA, the conditions in the co-spray and dip techniques are considerably different in that the solution for dip-immersion contains partially formed chains of polymer, while the polymer is presumably formed during deposition and for a short reaction period (1 min)

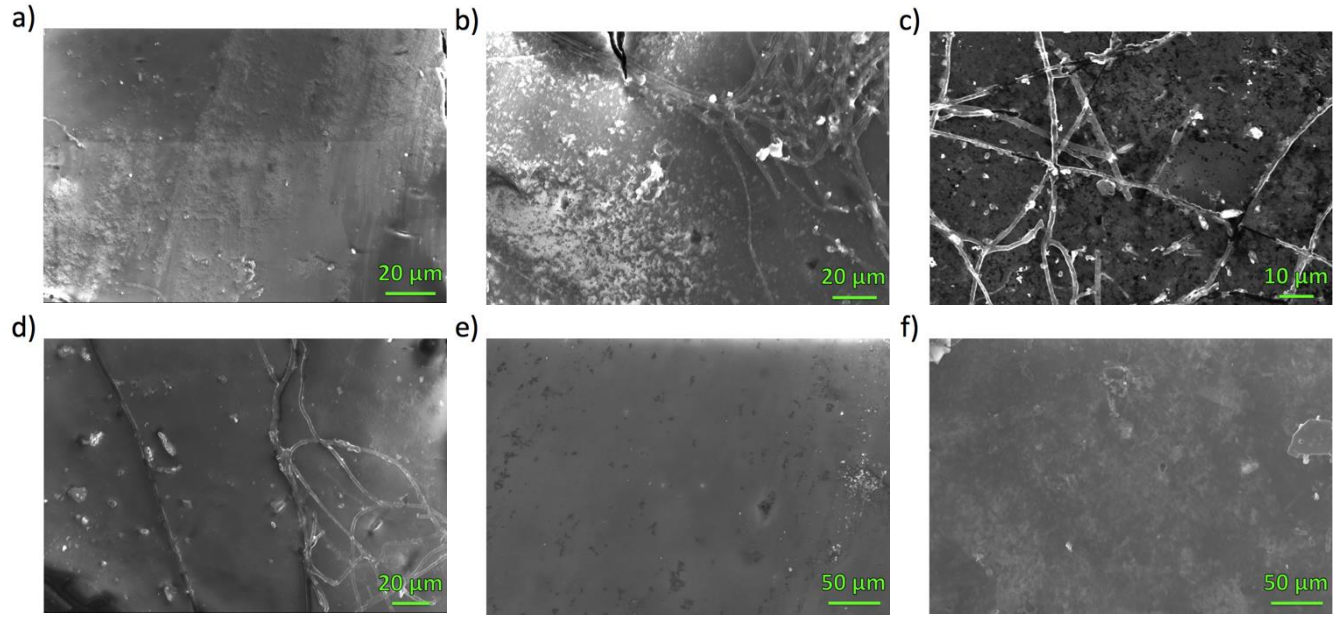

Figure 6. SEM images of a) bare anion-exchange membrane, and b) 2:3 dip 1 BL film, c) 2:3 dip 6 BL film, d) PEDOT-PMA film, e) 4:1 dip 1 BL and f) 4:1 dip 6 BL GO/PEDOT on anion-exchange membrane.

when co-sprayed. While the absorbance spectrometric data indicates the formation of multilayers with this method, it is possible that these conditions are not conducive to forming a single monolayer. This is in agreement with the low absorbance for films constructed using this method relative to the two dip methods, which imply predictable film growth is not possible until more BLs are attempted. It is possible that the polymerization process is not allowed to sufficiently progress to form useful material with this method compared to the presumably longer-chain PEDOT-PMA system produced in the metastable solutions used in the dip method.

BPMs containing varying loadings of GO/PEDOT were assembled using the co-spray method (Figure 7B). With the addition of 1 BL, the overpotential decreases markedly compared to the untreated BPM (2.7 V @ 20 mA/cm^2). With 2 and 4 BLs at the interface, the overpotential further decreases and the *J-E* trace resembles that of spin-coated GO. Therefore, in the presence of co-sprayed PEDOT, which was shown to be ineffective for WD, catalysis is dominated by the GO layers and the structure formed does not give superior efficiency compared to spin-coated GO. Increasing the interface from 4 to 6 BLs is detrimental to the overpotential, likely because the increased layer thickness suppresses ion transport.

When the deposition method was switched from spray to dip, first with the 2:3 EDOT:PMA recipe, WD on 1 BL GO/PEDOT considerably further improves upon the co-sprayed analog, with a lower overpotential than both the dipped PEDOT-PMA and spin-coated GO references (1.8 V @ 20 mA/cm^2) (Figure 7C). This observed synergy of GO and PEDOT implies that the dip-LbL deposition leads to a superior structure in terms of supporting WD. This is contradictory to the general preference of spray deposition to dip deposition,[33] and could be due to ineffective polymerization conditions in the co-spray method, as discussed. Whereas, the 2:3 dip method produces very inhomogeneous films, but the presence of PEDOT is detectable and plays a significant role in WD. It is also possible that the enhancement is associated with smoother, homogeneous films suggested by AFM that are co-generated with the GO flakes and polymer strings in the deposition as observed by SEM. Higher film loadings (2 – 6 BLs) yield higher overpotentials, but are still better than spin-coated GO (in the absence of PEDOT). Also notable are the relatively high limiting currents observed for BPMs made with this method that could be due to the rough, heterogeneous interface, which has been shown to strongly influence ion leakage.[19]

When the EDOT:PMA ratio was adjusted to 4:1, the overpotential is the same as the 2:3 dip method for 1 BL (Figure 7D). However, with higher film loadings the overpotential decreases further and is optimal with 2 and 4 BLs (1.5 V @20 mA/cm^2). Again, the synergistic behavior is demonstrated in a (dip) LbL-generated BPM interface, and this superior overpotential is congruent with the smooth, uniform morphology observed by AFM and SEM, and the predictable film growth observed by UV-visible spectroscopy. This phenomenon is contrary to the overpotentials observed for GO-only films deposited in different ways (Figure 7A), which suggest the resulting GO structure would not affect WD performance. Clearly, GO film assembly alongside PEDOT, which showed catalytic activity alone when deposited by dipping in the metastable solution, plays a critical role in BPM interface functionality.

Conclusions

Hybrid films of a conducting polymer and WD catalyst were deposited onto various substrates using variations of LbL methodology to optimize film quality by surveying the effect of polymerization conditions (concentration and concentration ratio)

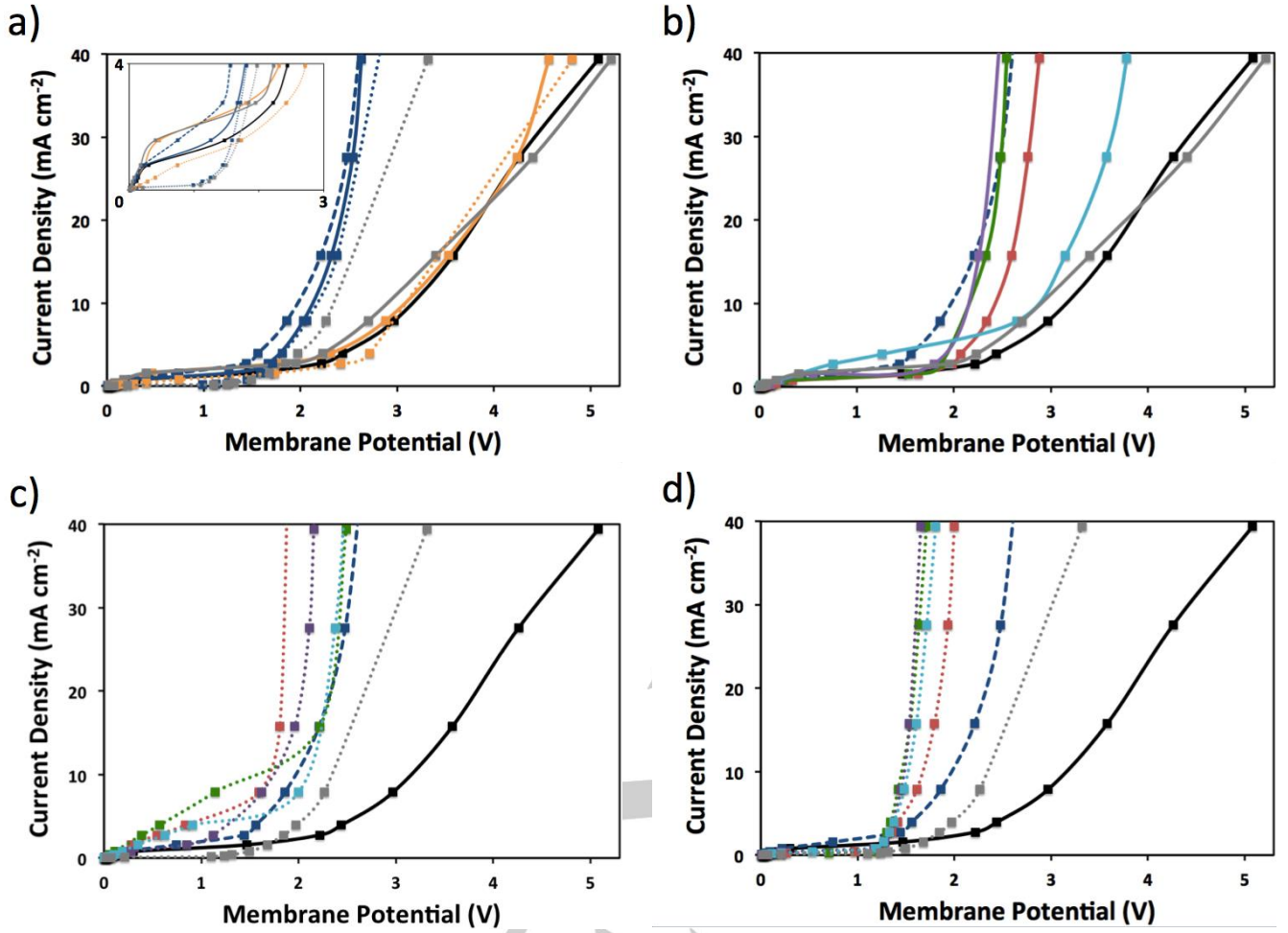

Figure 7. Comparison of *J-E* behavior for a) control, b) co-spray, and c) 2:3 and d) 4:1 EDOT:PMA dip-made BPM interfaces composed of PMA (orange), PEDOT-PMA (grey), GO (blue), and 0 BL (black), 1 BL (red), 2 BL (green), 4 BL (purple) and 6 BL (aqua) GO/PEDOT deposited by spray (solid), dip (dotted) and spin-coated (dashed) methods.

and exposure type (co-spray vs dip). Using UV-visible spectroscopy, it was found that films were successfully formed using these techniques, with the most predictable deposition using a 4:1 stoichiometric dip method. This 'rationalized' recipe, incorporating a monomer/oxidant ratio corresponding to the known final amount of PMA incorporated into the PEDOT-PMA system, also showed the most uniform films in both AFM and SEM examinations, compared to significant heterogeneity observed for co-spray and 2:3-dipped films. The controllability of layering is expected to be important for WD in BPM efficiency. XPS confirmed no presence of PMA in thinner films (< 10 BL), indicating genuine LbL growth by electrostatic binding between PEDOT and GO only, while there is a breakdown in predictable growth and incorporation of PMA for thicker layers, likely due to aging of the metastable solution resulting in PEDOT-PMA conglomeration. Through-plane conductivity measurements were carried out and reveal a membrane ohmic drop of ~100 mV, which is within aims for efficient membrane-integrated AP applications. Electrochemical evaluation on these systems in a BPM configuration shows that the method to deposit GO alone is irrelevant to WD overpotential, while it is shown that dip-deposition improves PEDOT-PMA WD overpotential. In all cases where the hybrid film deposited by LbL was tested, the performance was significantly better than the individual components regardless of deposition recipe (1.5 V vs 2.3 V and 2.7 V @20 mA/cm^2), indicating a synergistic effect between these components when combined in an alternating thin film system. This can be attributed to the improved control of molecular orientation and film formation afforded by the LbL methodology compared to spin-coating, which streamlines WD catalysis and product transport. This is most remarkable for BPMs modified using the 'rationalized' 4:1 dip deposition, which was shown in all cases to produce the highest quality films and therefore the highest quality electrochemical performance at 2 – 4 BL (~100 nm) thick. This combination of catalyst and conductor in a film tailored on the molecular level eliminates the tradeoff between WD efficiency and electron transport.

Experimental Section

Chemicals. GO aqueous solution (2 mg/mL), 3,4-ethylenedioxythiophene (EDOT, 97%), phosphomolybic acid hydrate (PMA) and reagent-grade acetonitrile were purchased from Sigma-

Aldrich and used without further purification. Water purified by in-house reverse osmosis was sourced for all experimental steps.

LbL Film Fabrication. Natively uncharged substrates such as glass (microscope slides, VWR) and Si (wafers, 1-0-0 orientation, N-doped, WaferPro) were initially cleaned with soap and water, dried under N_2 stream, and placed in a O_2 PDC-32G Plasma Cleaner (Harrick) at 400 mTorr for 15 min. The positively charged Neosepta AHA anion-exchange membrane (Ameridia) substrates were rinsed with water and dried in air without further treatment. Films were constructed on the substrate using the dip or co-spray methods illustrated in Scheme 1. For PEDOT-PMA baths, metastable solutions of PEDOT-PMA were made by first dissolving PMA in 25 mL of acetonitrile under brief sonication, followed by addition of EDOT in the ratios of 2:3 and 4:1 [EDOT]:[PMA]. For the dip methods, the baths containing GO were used as-received. Thinner films (≤ 6 bilayers) (BLs) were fabricated manually, while thicker films were fabricated automatically using a HMS Series Programmable Slide Stainer (Carl Zeiss) by immersing the substrate in the alternating baths of GO and PEDOT/PMA for 1 min, separated by two rinse steps (20 s and 10 s, respectively) in separate solvent-only baths (water for GO, acetonitrile for PEDOT-PMA), as many times necessary to achieve the desired number of BLs. For the co-spray method, a custom-built LbL spray instrument consisting of a rotating stage for the substrate and four airbrush nozzles controlled manually or by a programmable relay was used. Four nozzle-compatible containers, each with suction straws, were filled with: (1) a rinse solution of 50/50 v/v water/ acetonitrile; (2) as-received GO solution with pH adjusted to 11 using 1 M NaOH; (3) 100 mM EDOT in acetonitrile; and (4) 10 mM PMA in water with pH adjusted to 2 using 1 M H_2SO_4. The substrate was mounted on a PTFE rotating stage and the nozzles were sprayed in the cycle order of: GO, rinse, EDOT and PMA in concert, rinse, and was repeated as many times necessary to achieve the desired number of BLs. The approximate time for each spray was 5 – 10 s for the coating solutions, and 15 – 20 s for rinsing. After each EDOT/PMA spray, there was a 1 min pause to allow polymerization.

LbL Film Characterization. BL accumulation was monitored by intermittently measuring the UV-visible light absorbance of films deposited on glass substrates using a DU 800 spectrophotometer (Beckman Coulter). Atomic force microscopy (AFM) studies of films deposited on anion-exchange membrane were carried out on a Nanoscope V with a Dimension 3100 D3005-1 detector (Veeco) in tapping mode using a 6 N/m cantilever (Bruker). Scanning electron microscopy (SEM) of films on anion-exchange membrane utilized a 6010LA instrument (JEOL) with SEI detector at 20 kV. Film thicknesses were measured using a 633 nm wavelength variable angle ellipsometer (Gaertner Scientific) on FTO (on glass) substrates with the glass backside painted with red nail polish,[39] and assuming a thickness of 340 nm and an index of refraction of 2.4 for the specific FTO product used.[40] X-ray photoelectron spectroscopy (XPS) was collected on a Versaprobe II (Phi Physical Electronics) instrument. Electronic conductivities of films produced by the 4:1 dip method were measured by depositing the film on > 1 cm^2 of 1 × 3 cm FTO-glass substrates and clamping a pristine FTO-glass piece of the same dimensions perpendicularly to form a 1 cm^2 contact area. The exposed pristine FTO terminals were connected to a 263A Potentiostat/Galvanostat (Princeton Applied Research) in a 2-electrode configuration and voltage was scanned between 0 and 10 V (Figure S2). The slope of the resulting current-voltage relationships was used to derive the electrical resistance, and then used with the known/estimated dimensions of the film to calculate the conductivity values over several samples.

BPM Fabrication. In-house BPMs were fabricated similar to previously described.[9, 13] LbL-modified (and unmodified) anion-exchange membranes (4 × 4 cm) were fastened to glass substrates using electrical tape. A protective layer of Nafion (5 wt% in water/alcohols, Sigma-Aldrich) was spin-coated on the film at 2000 rpm for 5 min using a SCS 6800 Spin Coater (SCS Coatings) and heated at 100°C on a hotplate for 10 min. Following, several drops of Nafion solution (10 wt% in water, Sigma-Aldrich) were placed on the previous Nafion protective layer to form an adhesion layer with a fully hydrated, pre-formed Nafion NR-211 sheet (Ion Power Inc.), which was draped over the surface to form the cation-exchange side of the BPM. BPMs were dried overnight in ambient conditions.

Electrochemical Evaluation. BPMs were removed from the glass substrates and cut out of the electrical tape frame with shears. Membranes were placed between two symmetric custom glass chambers outfitted with Luggin capillaries and custom gaskets formed by casting liquid electrical tape on the flanges (Department of Chemistry Glass Shop, University of Manitoba), and bound tightly with a bar clamp to form an H-cell. Two platinum working electrodes were fabricated using 1 cm^2 Pt foil (0.05 mm, 99.9%, Sigma-Aldrich) fixed to copper wire with silver epoxy (Grainger), sealed in glass tubing with epoxy (Devcon), and placed in the outer H-cell chambers as current generators. Saturated calomel reference electrodes (CH Instruments) were placed in the inner Luggin compartments to measure membrane voltage. Both chambers were filled with 1 M $NaClO_4$ aqueous electrolyte and allowed to soak into the membranes for at least 5 hr. The current density-voltage relationship was discerned by passing galvanostatic currents using a 263A Potentiostat/Galvanostat (Princeton Applied Research) in increments of 30 min progressive steps between 0 and 80 mA/cm^2, corrected for an exposed membrane area of 2.54 cm^2, with 20 min breaks (no applied current) in between to equilibrate voltage.

Acknowledgements

This work was supported by NSF under the NSF CCI Solar Fuels Program under Grant No. CHE-1305124.

Keywords: bipolar membranes • layer-by-layer • artificial photosynthesis • solar fuels • graphene oxide • conducting polymers • PEDOT • heteropoly acid • phosphomolybdic acid

1. T. W. Xu, *Resour., Conserv. Recycl.* **2002,** *37*, 1-22.
2. R. Simons, *Electrochim. Acta* **1985,** *30*, 275-282.
3. P. Ramirez, H. J. Rapp, S. Reichle, H. Strathmann, S. Mafe, *J. Appl. Phys.* **1992,** *72*, 259-264.
4. H. Strathmann, *Desalination* **2010,** *264*, 268-288.
5. M. B. McDonald, S. Ardo, N. S. Lewis, M. S. Freund, *ChemSuSchem* **2014,** *7*, 3021-3027.
6. H. Gerischer, *J. Electroanal. Chem. Interfacial Electrochem.* **1977,** *82*, 133-143.
7. M. G. Walter, E. L. Warren, J. R. McKone, S. W. Boettcher, Q. X. Mi, E. A. Santori, N. S. Lewis, *Chem. Rev.* **2010,** *110*, 6446-6473.
8. R. Elmoussaoui, G. Pourcelly, M. Maeck, H. D. Hurwitz, C. Gavach, *J. Membr. Sci.* **1994,** *90*, 283-292.
9. M. B. McDonald, M. S. Freund, *ACS Appl. Mater. Interfaces* **2014,** *6*, 13790-13797.
10. H. B. Gray, *Nat. Chem.* **2009,** *1*, 7.
11. S. L. McFarlane, B. A. Day, K. McEleney, M. S. Freund, N. S. Lewis, *Energy Environ. Sci.* **2011,** *4*, 1700-1703.
12. J. Y. Liu, N. R. Davis, D. S. Liu, P. T. Hammond, *J. Mater. Chem.* **2012,** *22*, 15534-15539.
13. M. B. McDonald, J. P. Bruce, K. McEleney, M. S. Freund, *Chemsuschem* **2015,** *8*, 2645-2654.
14. J. Balster, S. Srinkantharajah, R. Sumbharaju, I. Punt, R. G. H. Lammertink, D. F. Stamatialis, M. Wessling, *J. Membr. Sci.* **2010,** *365*, 389-398.
15. S. Mafe, P. Ramirez, A. Alcaraz, *Chem. Phys. Lett.* **1998,** *294*, 406-412.

16. H. Strathmann, J. J. Krol, H. J. Rapp, G. Eigenberger, *J. Membr. Sci.* **1997,** *125*, 123-142.
17. K. Ariga, J. P. Hill, Q. M. Ji, *Phys. Chem. Chem. Phys.* **2007,** *9*, 2319-2340.
18. M. S. Kang, Y. J. Choi, S. H. Kim, S. H. Moon, *J. Membr. Sci.* **2004,** *229*, 137-146.
19. S. Abdu, K. Sricharoen, J. E. Wong, E. S. Muljadi, T. Melin, M. Wessling, *ACS Appl. Mater. Interfaces* **2013,** *5*, 10445-10455.
20. S. Mao, H. H. Pu, J. H. Chen, *RSC Advances* **2012,** *2*, 2643-2662.
21. P. T. Hammond *Adv. Mater.* **2004,** *16*, 1271-1293.
22. S. H. Lee, J. R. Harding, D. S. Liu, J. M. D'Arcy, Y. Shao-Horn, P. T. Hammond, *Chem. Mater.* **2014,** *26*, 2579-2585.
23. P. Podsiadlo, B. S. Shim, N. A. Kotov, *Coord. Chem. Rev.* **2009,** *253*, 2835-2851.
24. S. Correa, K. Y. Choi, E. C. Dreaden, K. Renggli, A. Shi, L. Gu, K. E. Shopsowitz, M. A. Quadir, E. Ben-Akiva, P. T. Hammond, *Adv. Funct. Mater.* **2016,** *26*, 991-1003.
25. M. S. Freund, B. A. Deore in *Self-Doped Conducting Polymers*. John Wiley & Sons, Ltd, Chichester, UK, **2007**, pp. 338.
26. S. Kirchmeyer, K. Reuter, *J. Mater. Chem.* **2005,** *15*, 2077-2088.
27. H. Shi, C. C. Liu, Q. L. Jiang, J. K. Xu, *Adv. Electron. Mater.* **2015,** *1*, 16.
28. D. Wakizaka, T. Fushimi, H. Ohkita, S. Ito, *Polymer* **2004,** *45*, 8561-8565.
29. A. M. Osterholm, J. F. Ponder, J. A. Kerszulis, J. R. Reynolds, *ACS Appl. Mater. Interfaces* **2016,** *8*, 13492-13498.
30. E. Bravo-Grimaldo, S. Hachey, C. G. Cameron, M. S. Freund, **2007,** *40*, 7166-7170.
31. S. L. McFarlane, B. A. Deore, N. Svenda, M. S. Freund, *Macromolecules* **2010,** *43*, 10241-10245.
32. M. B. McDonald, M. S. Freund, *ACS Appl. Mater. Interfaces* **2011,** *3*, 1003-1008.
33. A. Izquierdo, A.; S. S. Ono, J. C. Voegel, P. Schaaf, G. Decher, *Langmuir* **2005,** *21*, 7558-7567.
34. B. N. Balzer, S. Micciulla, S. Dodoo, M. Zerball, M. Gallei, M. Rehahn, R. von Klitzing, T. Hugel, *ACS Appl. Mater. Interfaces* **2013,** *5*, 6300-6306.
35. M. Unlu, J. F. Zhou, P. A. Kohl, *J. Phys. Chem. C* **2009,** *113*, 11416-11423.
36. S. Chabi, K. M. Papadantonakis, N. S. Lewis, M. S. Freund, *Energy Environ. Sci.* **2017,** *10*, 1320-1338.
37. F. G. Wilhelm, I. Punt, N. F. A. van der Vegt, M. Wessling, H. Strathmann, *J. Membr. Sci.* **2001,** *182*, 13-28.
38. D. E. Katsoulis, *Chem. Rev.* **1998,** *98*, 359-387.
39. R. A. Synowicki, *Phys. Status Solidi C* **2008,** *5*, 1085-1088.
40. K. vonRottkay, M. Rubi in *Optical indices of pyrolytic tin-oxide glass*, Symposium on Thin Films for Photovoltaic and Related Device Applications, Materials Research Society, San Francisco, CA, **1996**, pp. 449-454.

FULL PAPER

Michael B. McDonald, Michael S. Freund, Paula T. Hammond**

Page No. – Page No.

Catalytic, Conductive Bipolar Membrane Interfaces via Layer-by-Layer Deposition for the Design of Membrane-Integrated Artificial Photosynthesis Systems

Molecularly-tailored bilayers of catalytic graphene oxide and electronically conducting PEDOT demonstrate superior and synergistic water dissociation catalysis in the bipolar membrane interfacial layer, and provide opportunities in electronic applications such as membrane-integrated solar fuels generation.